

Detection of X-Ray Emission from the PSR 1259-63/SS2883 Binary System*

Lynn Cominsky[†]

Department of Physics and Astronomy, Sonoma State University, Rohnert Park, CA 94928
Stanford Linear Accelerator Center, Stanford University, Stanford, CA 94309
I: lynnc@charmian.sonoma.edu

Mallory Roberts

Department of Physics and Astronomy, Sonoma State University, Rohnert Park, CA 94928
I: mallory@charmian.sonoma.edu

and

Simon Johnston

Research Centre for Theoretical Astrophysics, University of Sydney, NSW 2006, Australia
I: simonj@physics.su.oz.au

ABSTRACT

Nonpulsed but variable X-ray emission has been detected from the binary system containing the radio pulsar PSR 1259-63 during two pointed ROSAT observations, taken five months apart. This 47.7 ms radio pulsar is in a highly eccentric ($\epsilon \sim .85$) binary system with the 10 to 15 M_{\odot} Be star SS2883. It is the first radio pulsar found to be in a binary system with a massive main sequence companion; it is also the most highly eccentric binary system known to contain a neutron star.

The level of X-ray flux detected in the ROSAT observations has increased with orbital phase by a factor of at least ten between 1992 February and 1993 February. The X-ray flux is significantly greater than expected from the Be star's corona and seems likely to originate either from low-level stellar wind accretion onto the neutron star or from the shock between the stellar wind and the relativistic pulsar wind. The system may be the progenitor of the more slowly rotating Be X-ray binary pulsar systems.

To appear in the Astrophysical Journal

*Work supported in part by Department of Energy contract DE-AC03-76SF00515 (SLAC) and by a grant from the NASA ROSAT Guest Observer Program, NAG 5-1684.

[†]Permanent address: Sonoma State University; Visiting Professor, Stanford Linear Accelerator Center.

1. Introduction

PSR 1259–63 was discovered in a radio survey of the southern galactic plane by Johnston et al. (1992a). Subsequent analysis (Johnston et al. 1992b) led to the identification of this 47.7 ms radio pulsar with the Be star SS2883, and on-going analysis of radio data has allowed the spin and orbital parameters to be determined to a high degree of precision (Johnston et al. 1993a,b). The pulsar has a relatively young characteristic age of 3×10^5 year and a moderate magnetic field strength of 3×10^{11} G. It is in a highly eccentric, 3.4 year orbit around the Be star.

PSR 1259–63 may be the progenitor of eccentric X-ray Be star binaries such as 4U0115+63 (Cominsky et al. 1978, Rappaport et al. 1978) and A0538–66 (Skinner et al. 1982). In the former system, strong X-ray outbursts are centered around periastron, but often last for more than one orbital cycle, while weaker ones occur near apastron, approximately 12 days later (Whitlock, Roussel-Dupré, and Priedhorsky 1989). In the latter system, the outbursts occur near each successive periastron, but only when the system is active. Both these systems have much shorter orbital periods and longer pulsation periods than does PSR 1259–63 (24.3 day and 3.6 s for 4U0115+63 and approximately 17 day and 69 ms for A0538–66).

By analogy to the other, more well-studied Be binaries, X-ray emission from this system may vary from low-level accretion of captured wind material away from periastron to a transient outburst nearer to periastron, when the pulsar more closely approaches the circumstellar envelope of the Be companion. It is also possible for the pulsar itself to produce pulsed X-rays in a manner similar to that of other young, nearby isolated neutron stars such as the Crab, and for SS2883 to produce weak coronal X-ray emission. Finally, the interaction of the winds from the pulsar and the companion could produce a shock front which could emit X-rays. These scenarios were considered in detail by Kochanek (1993), who concluded that the most copious source of X-radiation away from periastron should be coronal emission from SS 2883 at an approximate flux of $\sim 10^{31}$ ergs s^{-1} . The system was also modeled by King (1993), who used preliminary orbital elements to discuss some evolutionary considerations of the mass transfer.

In this paper, we report our detection of significant ($\sim 10^{33}$ ergs s^{-1}) X-ray emission post-apastron in the PSR 1259–63 system. Our observations cannot be easily explained by any of the standard scenarios, and are discussed in detail in the sections that follow.

2. Observations and Analysis

We have obtained $\sim 46 \times 10^3$ s of ROSAT Position Sensitive Proportional Counter (PSPC) data. Table 1 summarizes these observations, which occurred in two multiday periods (“obs1” and “obs2”) separated by ~ 5 months. Each observation period was further subdivided into many short (34 to 1758 s) Good Time Intervals (GTIs). The second observing period was sufficiently long that we could analyze each half of the observation separately (“obs2a” and “obs2b”).

The ROSAT PSPC images produced by the Standard Analysis Software System (SASS) clearly indicate a source at a position consistent with PSR 1259–63. For the first observation period, the difference in the best-fit ROSAT SASS (version 5.8) position and the radio position (Johnston et al. 1992b) is $6''.9$, while for the second observation period (using SASS version 6.2) it was $9''.8$. Both of these position offsets are within the expected systematic uncertainties for

the PSPC ($15''$, 90% probable error radius). Images of PSR 1259–63 in both observation periods are consistent with a point source. There are no other objects listed in either SIMBAD or the Space Telescope Science Institute Guide Star Catalog (version 1.1) within this error region. In all observations, the location of PSR 1259–63 within the field of view occurs in a region with nonvarying exposure and background. Also within the (1° square) PSPC image, but well outside of the error region considered for PSR 1259–63, is a very bright X-ray source consistent in location with the G star HD113466. This star is present in both observation periods, as are several weaker, as yet unidentified objects. HD113466 is present in all three SASS images (0.1 to 0.7 keV, 0.7 to 2.4 keV, and 0.1 to 2.4 keV), while PSR 1259–63 is only present in the two images which include the more energetic photons.

In order to determine the intensity of the X-ray emission from the PSR 1259–63 system, we used the Post-Reduction Off-Line Software package (PROS version 2.10.2) and chose a circular integration region which had a radius of $100''$ around the fitted source position. The background was computed in an annular region with inner radius of $110''$ and outer radius of $210''$. The results from this analysis are given in Table 1.

The distance to the system is somewhat uncertain. The distance determination based on the pulsar’s dispersion measure was initially 2.3 kpc (Lyne, Manchester, and Taylor 1985) with stated uncertainties occasionally as large as a factor of 2. A more recent dispersion measure model, believed to be accurate for most pulsars to within 25%, yields a distance of 4.6 kpc for the system (Taylor and Cordes 1993). However, using optical photometry and the spectral type of the companion, Johnston et al. (1993b) find the distance to be ~ 1.5 kpc, and we therefore adopt this conservative value for use in further discussion. The X-ray luminosity in the PSPC 0.1 to 2.4 keV band that is required to explain our observed count rates is at least 6×10^{32} ergs s^{-1} and may be as high as 1×10^{34} ergs s^{-1} , depending on the assumed spectral model (see Sections 2.2 and 3.1 below for further details of this calculation.)

Pre-apastron ROSAT PSPC observations of PSR 1259–63 which occurred on 1992 February 26 were carried out for $\sim 7 \times 10^3$ s by M. Bailes and M. Watson (private communication). Fewer than 10 photons were detected from the system during this time, and we include the upper limit derived from these observations in Table 1. This upper limit is approximately a factor of 10 less than our detections at post-apastron orbital phases. The system was also observed prior to apastron using the Ginga LAC on 1991 September 5 (MJD 48505). T. Makino and T. Aoki (private communication) have found an upper limit for these observations of 0.1 mCrab (2 to 10 keV), equivalent to an X-ray luminosity of $\sim 6 \times 10^{32}$ ergs s^{-1} (assuming a Crab like spectrum). Upper limits derived from all sky surveys (Uhuru, Forman et al. 1978 and HEAO A-1, Wood et al. 1984) are about a factor of 20 higher than the Ginga LAC limit. Figure 1 depicts the orbital locations of the Ginga observation and the three sets of ROSAT observations.

2.1. Timing Analysis

As can be seen from the intensity information in Table 1, the overall flux from PSR 1259–63 has increased by at least a factor of ten between the Bailes et al. observations in 1992 February and our observations, and by an additional $\sim 50\%$ between our first and second observation periods, which are separated by about five months (obs1 occurred 1992 August 30–September 4, while obs2 occurred 1993 February 7–16). We have also searched for variability on shorter timescales by

computing the average flux per GTI. The results of this analysis indicate possible variations on timescales of a few hours. The variability is especially significant within the first half of obs2.

We have searched for X-ray pulsations at the 47.7 ms radio pulse period by performing the following analysis:

- (1) The individual photon times were extracted from the ROSAT FITS file and were converted from the spacecraft clock time to UTC.
- (2) We used PROS to generate a barycentric correction table, assuming the radio pulsar position given by Johnston et al. (1992b).
- (3) The individual photon arrival times were corrected to the solar system barycenter using a linear interpolation of the correction table.
- (4) A timing correction for the pulsar orbit (F_{orb}) was calculated for each arrival time using the orbital elements given in Johnston et al. (1993b).
- (5) Using the radio determined P and \dot{P} , the pulse number and phase were then calculated from the arrival time equation

$$t_{\text{arr}} = t_0 + NP + \frac{1}{2} N^2 P \dot{P} + \frac{a \sin i}{c} F_{\text{orb}}(\theta, \omega, \epsilon, \tau)$$

and a binned phase histogram was constructed.

No significant pulsed emission has been detected in either observation period, nor in the entire data set. Three sigma upper limits to the pulsed fraction are 21%, 9%, and 9% for obs1, obs2, and the entire dataset respectively. Additional searches using only the higher or lower energy bands (channels 10–100 or 100–255) also did not reveal any significant pulsed fraction.

2.2. Spectral Analysis

We have fitted power law, thermal bremsstrahlung, and Raymond-Smith spectra to the data from the PSR 1259–63 system. The photons were binned into 34 channels by PROS and fitted using XSPEC 8.30. In order to obtain acceptable fits, we had to eliminate low-energy channels 1 and 2, as there was no significant flux in these channels. In addition, channel 31 was eliminated for obs1 since it had an anomalously low flux. The results of our spectral fitting are summarized in Table 2 for obs1, obs2, and both halves of this longer observation period (obs2a and obs2b). For PSR 1259–63, we cannot discriminate between these three models based on goodness of fit, and we found no need to include any additional model components, as the simple fits were adequate. There is no significant metal abundance in the best-fit Raymond-Smith model.

We have also fitted spectra for the bright G star, which has significant soft X-ray emission, typical of a coronal plasma. These results are also given in Table 2, where it can be seen that the Raymond-Smith model is clearly preferred. The best-fit metal abundance (relative to cosmic) in this latter model is 0.14, which is not unreasonable for a Population II object.

We have performed a color-color analysis for the PSR 1259–63 data in the manner of Meurs et al. (1992), who analyzed many ROSAT observations of O and B stars, including some with and without emission lines. We find that, using their scheme, the colors for PSR 1259–63 are strikingly similar to those of X Per, a known accreting Be binary. The color-color ratios are 0.97 ± 0.04 and 0.67 ± 0.03 for the ratio of the (0.4–2.4 keV) to (0.1–2.4 keV) and the (1.0–2.4 keV) to (0.4–2.4 keV) energy bands, respectively.

3. Discussion

In order to account for the X-ray emission we have observed from the PSR 1259–63 system near apastron, we consider four different types of scenarios: coronal emission from the Be star companion, low-level accretion onto the neutron star, rotational spin-down energy from the neutron star and emission from interacting winds. In the sections that follow, we discuss the applicability of each scenario.

3.1. Be Star Coronal Emission

We assume that the bolometric luminosity of the companion star SS2883 is $5.8 \times 10^4 L_{\odot}$ (Westerlund and Garnier 1989, Johnston et al. 1992b). Using the relationship derived for B star coronal emission, $L_x = 1.4 \times 10^{-7} L_{\text{bol}}$ (Pallavicini et al. 1981), we obtain a predicted L_x of around 3×10^{31} ergs s⁻¹ (cf. Kochanek 1993). This relationship holds for the (0.1 to 4.5 keV) Einstein band and is consistent with that recently derived for (0.1 to 2.4 keV) ROSAT PSPC observations of other B and Be stars (Meurs et al. 1992).

For the assumed 1.5 kpc distance, and given the predicted intrinsic coronal luminosity of $\sim 3 \times 10^{31}$ ergs s⁻¹ and average observed spectrum, we calculate observed count rates per second (between 0.1 and 2.4 keV) of approximately 2.30×10^{-4} (Raymond-Smith model), 0.443×10^{-4} (power law model), and 1.60×10^{-3} (thermal bremsstrahlung model). We have observed count rates of $2.38 \pm 0.18 \times 10^{-2}$ (during obs1) and $3.15 \pm 0.11 \times 10^{-2}$ (during obs2). Therefore, our observed count rates are from 15 to 700 times higher than those expected from coronal emission. In addition, the spectral similarity between PSR 1259–63 and the known accreting neutron star binary X Per also argues against associating the observed X-ray emission with the companion star’s corona. It is therefore difficult to attribute the observed X-ray flux to coronal emission from SS2883.

3.2. Accretion Powered Emission

In systems such as PSR 1259–63, where the companion star lies well within its Roche lobe, accretion typically occurs as a result of the capture of radiatively driven stellar wind material by the neutron star. Alternatively, in a highly eccentric orbit, the companion star may temporarily fill its Roche lobe at periastron, providing an additional source of material to be accreted (Charles et al. 1983). In Be systems, the occasional ejection of circumstellar shell material may catalyze the accretion process and initiate a transient outburst as the shell reaches the neutron star. In all three of these scenarios, however, the accreting material will not be able to penetrate the magnetospheric boundary if it lies outside the corotation radius, and will be propelled away in a manner known as “centrifugal inhibition” (Stella, White, and Rosner 1986).

In addition, for rapidly rotating radio pulsars, the pressure exerted by the radio pulsar on the companion’s stellar wind should further inhibit the accretion process (Illarionov and Sunyaev 1975; Stella et al. 1986). It is possible for accretion to overcome both the centrifugal and the radio inhibition barriers if the magnetic field strength is low, and the wind density is high but with fairly low velocity (e.g., captured material piled up outside the magnetospheric boundary). For PSR 1259–63 rotating with a period of 47 ms, and an observed luminosity of at most 1×10^{34} ergs

s^{-1} , accretion would be possible; e.g., if the pulsar’s magnetic dipole is less than $5 \times 10^{26} \text{ G cm}^3$ ($B \sim 10^8 \text{ G}$), and the wind velocity $v_o = 2 \times 10^6 \text{ cm s}^{-1}$. However, the period derivative value reported by Johnston et al. (1993b) indicates that the magnetic field in this system is $3.3 \times 10^{11} \text{ G}$, and thus the X-ray luminosity we observe cannot be easily explained by the standard centrifugally inhibited accretion scenario.

However, if the centrifugal and radio pulsar inhibition mechanisms are not completely effective at stopping the infall of captured material (e.g., a fortuitous alignment of the field lines and the wind allows some matter to accrete), it may be possible to produce the low level luminosity that we have observed. If we assume that the pulsar is orbiting in the equatorial wind region of the Be star, then given the orbital parameters and stellar rotation velocity derived by Johnston et al. (1993b), and reasonable assumptions about the stellar wind velocity and density (Waters et al. 1989), the direct stellar wind capture scenario detailed by Waters et al. (1989) can re-create the observed X-ray flux increase with orbital phase. The model predicts only low-level emission before apastron, and then a maximum flux shortly after apastron, similar to our observations. It further predicts a lower luminosity at periastron due to the higher relative velocity of the neutron star and the stellar wind. The spectral similarity to X Per, a known low-luminosity accreting neutron star binary, offers additional support to the accretion scenario, despite the problems with centrifugal inhibition discussed above.

Charles et al. (1983) have proposed a temporary Roche lobe overflow scenario to explain observations of outbursts in A0538–66. These outbursts occurred regularly for a number of ~ 17 day cycles in the 1977 to 1982 era (Skinner et al. 1980, Corbet et al. 1985), but have not been reported during the past ~ 10 year. Using the recent orbital elements for PSR 1259–63 (Johnston et al. 1993b), we find that periastron passages in the system have occurred seven times since the earliest days of satellite based X-ray observations. Table 3 summarizes the predicted periastron times, and satellites with all-sky monitors which were observing at each date. No outbursts or detections have been reported from any of these observations. Upper limits to the outburst intensity for the Vela observations are 25 mCrab ($\sim 10^{35} \text{ ergs s}^{-1}$, 1σ) for a 10-day outburst or 250 mCrab ($\sim 10^{36} \text{ ergs s}^{-1}$, 3σ) for a 1 day outburst (Whitlock, private communication). The upper limits for the Hakucho and Ginga All Sky Monitors are ~ 100 mCrab and ~ 50 – 70 mCrab, respectively (H. Tsunemi, private communication). Typical X-ray transient outbursts in Be binaries have intensities ranging from 10^{36} to $10^{37} \text{ ergs s}^{-1}$ (van den Heuvel and Rappaport 1987) marginally consistent with these archival upper limits. The long orbital period in the PSR 1259–63 system limits the opportunities to observe periastron passage compared to the much shorter cycle in A0538–66, and the system may have been similarly inactive, or may have outbursts which are much fainter. In any event, since this mechanism is believed to produce X-ray emission only near periastron, it is not directly applicable to the observations reported in this paper.

The fast spin rate and high eccentricity in the PSR 1259–63 system seem to indicate that the system was recently created from the supernova event and is still spinning rapidly. Given the relationship between the orbital period and spin period of X-ray pulsars in Be binaries (Corbet 1984), we might expect this pulsar to eventually spin down to a much longer period. The physical mechanism that operates to slow down the neutron star is not clear, but scenarios which invoke braking in the companion’s wind are often proposed (e.g., Illarionov and Sunyaev 1975). This effect should be most pronounced at periastron, when the pulsar moves through the densest regions of the stellar wind. However, transient X-ray outbursts occurring as a result of periastron passage

in the 4U0115+63 system show the pulsar spinning up due to accretion (Rappaport et al. 1978). It is therefore important to study the PSR 1259–63 system during its next expected periastron passage near 1994 January 9. If the PSR 1259–63 system is to evolve into a more circular, slowly rotating system such as 4U0115+63, any accretion-driven spin-up during periastron must be countered by an efficient braking interaction during the rest of the pulsar’s very long orbit (e.g., propellar mechanism or radio pulsar spin-down.) The unexpected X-ray emission that we observe may be the result of this interaction.

3.3. Rotationally Produced X-Ray Emission

A few radio pulsars have also been detected as pulsed X-ray sources. These include not only the young pulsars such as the Crab and PSR 1509–58, but also recycled pulsars such as PSR 0437–4715. High-energy emission from the Crab has been modeled by many authors, and usually involves consideration of either the “polar cap model” (e.g., Daugherty and Harding 1982) or the “outer gap model” (e.g., Cheng, Ho, and Ruderman 1986). Recent calculations of these models have considered not only young pulsars like the Crab, but recycled pulsars as well (for example, see Chiang and Romani 1992 and references therein). These calculations show that young pulsars are expected to have a higher proportion of high energy emission than older pulsars. For the Crab, approximately 10% of the spin-down luminosity is radiated in the ROSAT band (Harnden and Seward 1984), and the pulsar’s luminosity is $\sim 4\%$ of this total. For PSR 1259–63, using the period derivative 2×10^{-15} (Johnston et al. 1993b) and a typical I of 10^{45} g cm², leads to an $\dot{E} = I\omega\dot{\omega}$ of $\sim 10^{36}$ ergs s⁻¹. Therefore, in this scenario, $\sim 10^{35}$ ergs s⁻¹ should appear as X-ray emission in the ROSAT band, with $\sim 4 \times 10^{33}$ ergs s⁻¹ as pulsed emission. As discussed above, the total X-ray luminosity we observe is less than $\sim 10^{34}$ ergs s⁻¹. If this system is producing pulsed X-ray emission, it must be at less than 0.1% of the spin-down energy, much lower than other pulsars with similar P and \dot{P} (e.g., PSR 1055–52, Ogelman and Finley 1993). This, coupled with the variability in flux by more than an order of magnitude and the lack of detected pulsations at the radio period, argues against rotationally powered X-ray emission.

3.4. Emission from Shocked Winds

As discussed in detail by Kochanek (1993), if the stellar and pulsar winds interact, shocks should occur between the two stars. The shocked stellar wind should radiate X-rays due to thermal bremsstrahlung. The X-ray luminosity expected in this case is a sensitive function of the ratio of the strength of the stellar wind to that of the pulsar (λ). In his model, λ is assumed to be much greater than one, and the calculated emission from the stellar wind shock would be a factor of 5 to 10 less than the expected coronal emission (see above). However, the pulsar wind should also be shocked, and it is not clear how the available energy in this shock (which comes from the pulsar’s spin-down energy and is potentially much greater) will emerge. For values of $\lambda \leq 20$, it seems possible to release as much energy as we have observed (see Figure 6 in Kochanek 1993.) Soft X-rays observed from PSR 1957+20 (Kulkarni et al. 1992, Fruchter et al. 1992) are consistent with this scenario; however, this system is very compact compared to PSR 1259–63, and the observed ROSAT flux was at least a factor of 10 (and possibly a factor of 10^3) lower than observed here. In support of this model are the observed X-ray flux increase as the neutron star approaches the companion star, the lack of strong X-ray pulsations, and the variability on short timescales.

4. Conclusions

We have detected variable, low-level, unpulsed X-ray emission from the PSR 1259–63 binary system which may result from low-level accretion or the interaction of the pulsar and Be star companion winds. X-ray emission from this system has increased by a factor of ten between 1992 February and 1993 February, and may continue to increase through 1994 January, when the neutron star most closely approaches its companion. The unique properties of this system offer an excellent opportunity to test theories of X-ray binary evolution, and we urge continued multiwavelength observations.

Acknowledgments

We are grateful to J. van Paradijs, S. Kulkarni, R. Romani, M. Walker, and A. King for useful discussion regarding possible X-ray emission mechanisms. We also thank M. Bailes and M. Watson for their analysis of the upper limit from the 1992 February ROSAT observations, F. Makino and T. Aoki for determining the Ginga LAC upper limit, L. Whitlock for information regarding the Vela upper limits, and H. Tsunemi for information about the Hakucho, Tenma, and Ginga All-Sky Monitor observations. H. Ogelman provided valuable assistance in the interpretation of the ROSAT barycentering data.

This research has made use of the SIMBAD database, operated at CDS, Strasbourg, France. This research has also made use of data obtained through the High Energy Astrophysics Science Archive Research Center online service, provided by the NASA Goddard Space Flight Center. LRC acknowledges the hospitality of the Particle Astrophysics group at the Stanford Linear Accelerator Center during part of this work.

REFERENCES

- Charles, P., et al., 1983, MNRAS, 202, 657
- Cheng, K. S., Ho, C., and Ruderman, M., 1986, ApJ, 300, 522
- Chiang, J., and Romani, R., 1992, ApJ, 400, 629
- Cominsky, L., Clark, G.W., Li, F., Mayer, W., and Rappaport, S., 1978, Nature, 273, 367
- Corbet, R., 1984, A&A, 141, 91
- Corbet, R., Mason, K. O., Córdoba, F. A., Branduardi-Raymont, G., and Parmar, A. N., 1985, MNRAS, 212, 565
- Daugherty, J. K., and Harding, A. K., 1982, ApJ, 252, 337
- Forman, W., Jones, C., Cominsky, L., Julien, P., Murray, S., Peters, G., Tananbaum, H., and Giacconi, R., 1978, ApJS, 38, 357
- Fruchter, A. S., Bookbinder, J., Garcia, M. R., and Bailyn, C. D., 1992, Nature, 359, 303
- Harnden, F. R. and Seward, F. D., 1984, ApJ, 283, 279
- Illarionov A.F., and Sunyaev R.A., 1975, A&A, 39, 185
- Johnston, S., Lyne, A.G., Manchester, R.N., Kniffen, D. A., D’Amico, N., Lim, J., and Ashworth, M., 1992a, MNRAS, 255, 401
- Johnston, S., Manchester, R.N., Lyne, A.G., Bailes, M., Kaspi, V.M., Qiao, G., and D’Amico, N., 1992b, ApJ, 387, L37
- Johnston, S., Manchester, R., Lyne, A., and D’Amico, N., 1993a, IAU Circular 5794
- Johnston, S., Manchester, R. N., Lyne, A. G., Nicastro, L., and Spyromilio, J. 1993b, MNRAS, submitted
- King, A. R., 1993, ApJ, 405, 727
- Kochanek, C., 1993, ApJ, 406, 638
- Kulkarni, S. R., Phinney, E. S., Evans, C. R., and Hasinger, G., 1992, Nature, 359, 300
- Lyne, A. G., Manchester, R. N., and Taylor, J. H., 1985, MNRAS, 213, 613
- Meurs, E. J. A. et al., 1992, A&A, 265, L41
- Ogelman, H. and Finley, J. P., 1993, ApJ, 413, L31
- Pallavicini, R., Golub, L., Rosner, R., Vaiana, G. S., Ayres, T., and Linsky, J. L., 1981, ApJ, 248, 279
- Rappaport, S., Clark, G. W., Cominsky, L., Joss, P. C., and Li, F., 1978, ApJ, 211, L1

- Skinner, G. K., et al., 1980, *ApJ*, 240, 619
- Skinner, G. K., Bedford, D. K., Elsner, R. F., Leahy, D., Weisskopf, M. C., and Grindlay, J., 1982, *Nature*, 297, 568
- Stella, L., White, N.E., and Rosner, R., 1986, *ApJ*, 308, 669
- Taylor, J. H. and Cordes, J. M., 1993, *ApJ*, 411, 674
- van den Heuvel, E. P. J. and Rappaport, S., 1987, *Physics of Be Stars: Proceedings of the 92nd Colloquium of the International Astronomical Union, Boulder, Colorado, 18–22 August 1986*, A. Slettebak and T. D. Snow, New York: Cambridge University Press, 291
- Waters, L. B. F. M., de Martino, D., Habets, G. M. H. J., and Taylor, A. R., 1989, *A&A*, 223, 207
- Westerlund, B. E. and Garnier, R., 1989, *A&AS*, 78, 203
- Whitlock, L., Roussel-Dupré, D. and Priedhorsky, W., 1989, *ApJ*, 338, 381
- Wood, K., et al., 1984, *ApJS*, 56, 507

TABLE 1
INTENSITY AND VARIABILITY SUMMARY FOR PSR 1259–63

| Interval | MJD | GTIs | Source Photons | Duration (s) | Flux $\times 10^{-2}$ counts s^{-1} | χ^2 |
|----------|---------------------|------|---------------------|-----------------|---|----------|
| Bailes | 48678.68–48679.78 | | < 10 | 7086 | < 0.26 (99% C.L.) | |
| obs1 | 48864.527–48869.167 | 10 | 253.8 ± 18.88 | 10713 | 2.38 ± 0.18 | 1.03 |
| obs2 | 49025.895–49034.539 | 34 | 1135.86 ± 37.89 | 36108 | 3.15 ± 0.11 | 1.66 |
| obs2a | 49025.895–49029.823 | 13 | 499.99 ± 25.12 | 14133 | 3.54 ± 0.18 | 2.49 |
| obs2b | 49030.736–49034.539 | 21 | 635.87 ± 28.36 | 21975 | 2.91 ± 0.13 | 1.08 |

TABLE 2a
POWER LAW SPECTRAL FITS FOR PSR 1259–63

| Dataset | α | 90% C.L. | $N_H \times 10^{21}$ | 90% C.L. | Norm $\times 10^{-4}$ | χ^2 (dof) |
|---------|----------|-----------|----------------------|------------|-----------------------|----------------|
| obs1 | 3.74 | 1.59–6.86 | 6.68 | 2.43–13.32 | 6.61±5.01 | 30.18 (28) |
| obs2 | 2.16 | 1.42–3.00 | 3.83 | 2.34–5.58 | 3.95±1.09 | 32.80 (29) |
| obs2a | 1.56 | 0.54–2.81 | 2.57 | 0.68–5.14 | 3.03±1.19 | 37.83 (29) |
| obs2b | 3.03 | 1.98–4.29 | 5.61 | 3.43–8.34 | 5.90±2.42 | 17.43 (29) |
| G star | 2.28 | 2.18–2.37 | 0.36 | 0.33–0.39 | 11.01±0.19 | 338.89 (29) |

TABLE 2b
THERMAL BREMSSTRAHLUNG SPECTRAL FITS FOR PSR 1259–63

| Dataset | kT (keV) | 90% C.L. | $N_H \times 10^{21}$ | 90% C.L. | Norm $\times 10^{-4}$ | χ^2 (dof) |
|---------|------------|------------|----------------------|-----------|-----------------------|----------------|
| obs1 | 0.77 | 0.72–6.90 | 4.77 | 2.45–8.86 | 10.85±16.95 | 30.30 (28) |
| obs2 | 2.19 | 1.09–12.87 | 3.16 | 2.14–4.33 | 3.16±1.85 | 32.94 (29) |
| obs2a | 8.12 | 0.1–200.0 | 2.28 | 1.31–4.01 | 1.35±1.59 | 37.87 (29) |
| obs2b | 1.06 | 0.60–2.72 | 4.33 | 2.88–6.13 | 8.04±6.54 | 17.43 (29) |
| G star | 1.01 | 0.93–1.10 | 0.24 | 0.22–0.26 | 22.56±1.62 | 239.07 (29) |

TABLE 2c
RAYMOND-SMITH SPECTRAL FITS FOR PSR 1259–63

| Dataset | kT (keV) | 90% C.L. | $N_H \times 10^{21}$ | 90% C.L. | Norm $\times 10^{-4}$ | χ^2 (dof) |
|---------|------------|------------|----------------------|------------|-----------------------|----------------|
| obs1 | 1.13 | 1.08–9.33 | 3.90 | 1.15–17.18 | 13.81±26.46 | 30.02 (27) |
| obs2 | 2.61 | 2.60–14.56 | 3.01 | 2.18–4.33 | 14.38±9.40 | 33.02 (28) |
| obs2a | 6.09 | 6.08–79.90 | 2.42 | 1.39–4.02 | 12.84±9.96 | 37.90 (28) |
| obs2b | 1.05 | 0.49–2.77 | 4.33 | 2.83–11.02 | 26.87±25.87 | 17.43 (28) |
| G star | 0.84 | 0.81–0.86 | 0.15 | 0.14–0.17 | 45.08±2.70 | 58.41 (28) |

TABLE 3
PSR 1259–63 PERIASTRON PASSAGE OBSERVATIONS
WITH ALL-SKY MONITORS

| Date of Periastron | MJD | Satellite |
|--------------------|----------|----------------|
| 1970 Apr 27 | 40703.52 | <i>Vela</i> |
| 1973 Sep 15 | 41940.33 | <i>Vela</i> |
| 1977 Feb 3 | 43177.14 | <i>Vela</i> |
| 1980 Jun 23 | 44413.94 | <i>Hakucho</i> |
| 1983 Nov 12 | 45650.75 | None* |
| 1987 Apr 2 | 46887.55 | <i>Ginga</i> |
| 1990 Aug 21 | 48124.36 | <i>Ginga</i> |

*Although Tenma was operational during this time,
PSR 1259–63 was not in the field of view of the
All-Sky Monitor (Tsunemi, private communication).

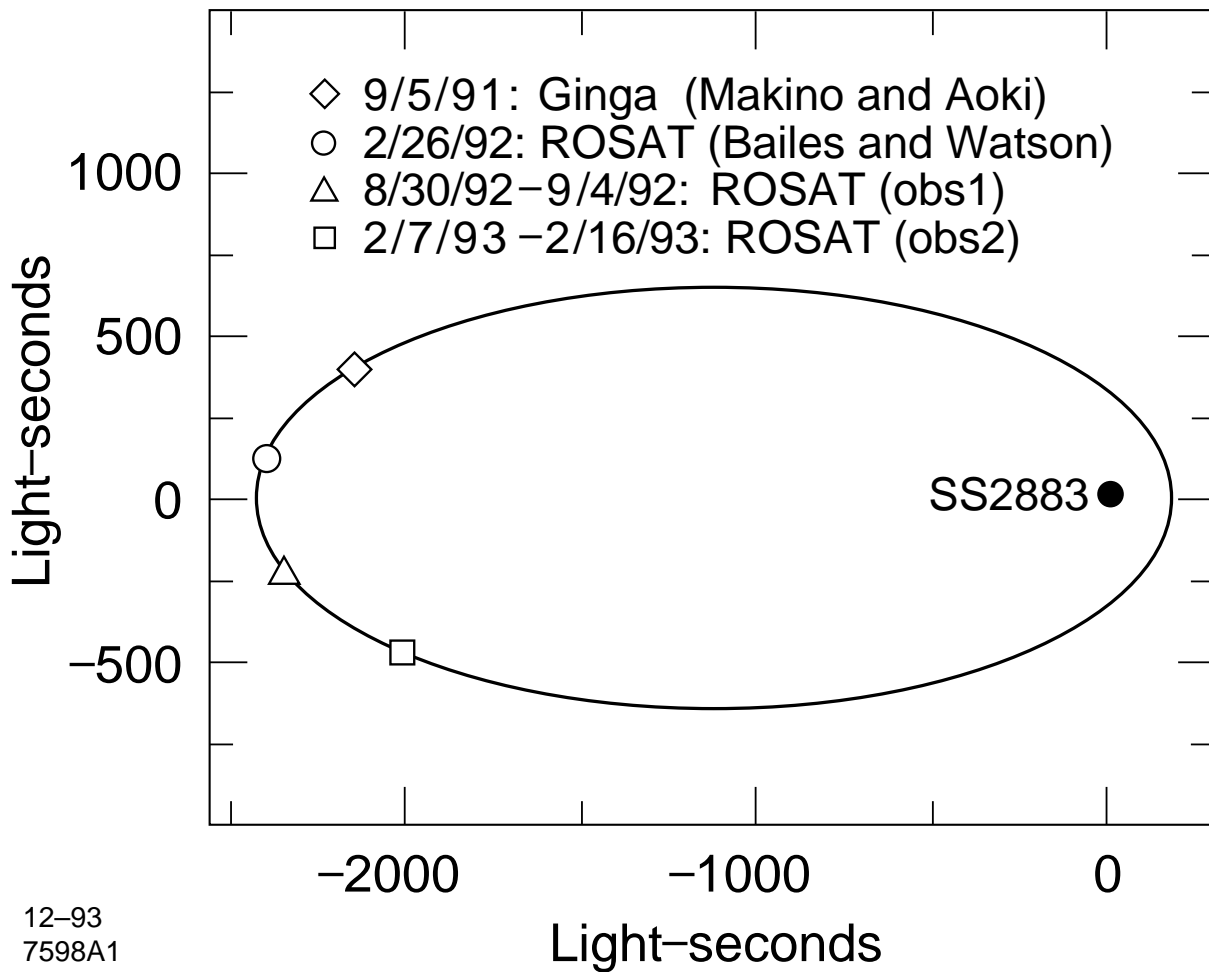


Fig. 1. Schematic of the orbit of PSR 1259-63, in which the companion, SS2883, is placed at the center-of-mass of the system. Also indicated are the pre-apastron observations using the Ginga LAC (Makino and Aoki) and ROSAT PSPC (Bailes and Watson) which resulted in upper limits, as well as our ROSAT PSPC observations, obs1 and obs2.